AIMS Materials Science, 5(5): 1000–1015.
DOI: 10.3934/matersci.2018.5.1000
Received: 21 August 2018
Accepted: 23 October 2018
Published: 29 October 2018

http://www.aimspress.com/journal/Materials

Research article

The use of various peening methods to improve the fatigue strength of titanium alloy Ti6Al4V manufactured by electron beam melting

Hitoshi Soyama* and Yuya Okura

Department of Finemechanics, Tohoku University, 6-6-01 Aoba, Aramaki, Aoba-ku, Sendai, Miyagi, 980-8579, Japan

*** Correspondence:** Email: soyama@mm.mech.tohoku.ac.jp; Tel: +81227956891.

Abstract: Additive manufacturing (AM) of metals is one of the foremost methods used for making medical implants and components for aviation. However, the fatigue strength of AM metals is weaker than that of the bulk equivalent. Mechanically treating the surface, such as by shot peening, can improve the fatigue strength, and novel peening methods without shot have also been proposed. In this paper, in order to demonstrate the improvements made in AM metals by various peening methods, specimens made of titanium alloy Ti6Al4V manufactured by electron beam melting (EBM) were treated by shot peening, laser peening and cavitation peening, then assessed by a plate bending fatigue test. In the case of shot peening, the shots were accelerated by a water jet to mitigate the incidence of dust during the process. For laser peening, the specimen was placed in water, and the effect of the impact produced at the target due to collapsing bubbles, which developed after laser ablation of the surface, was greater than the effect due to the laser ablation itself. For cavitation peening, the cavitation was generated by injecting a high speed water jet into water. In each case improvements in the fatigue strength of the Ti6Al4V were made. Improvements of 104% by laser peening, 84% by cavitation peening and 68% by shot peening compared with a non-peened specimen were achieved.

Keywords: mechanical surface treatment; medical implant; titanium alloy; additive manufacturing; electron beam melting; fatigue strength; shot peening; laser peening; cavitation peening

1. Introduction

Additive manufacturing (AM) of metals is an attractive process for manufacturing medical

implants and aviation components, in the first case because it is easy to make implants that are an order more porous [1] and in the second case because the weight of components can be reduced by the increased design freedom without having to consider machining [2]. Unfortunately, the fatigue strength of AM metals is significantly less than that of their bulk counterparts [2,3]. It has been reported that mechanically treating the surface, such as by shot peening, can improve the fatigue strength of AM metals [2,3]. However, a comparison between the improvements made to the fatigue strength of AM metals by conventional shot peening and novel peening methods, such as laser peening [4–6] and cavitation peening [7], has not been done. Therefore, we carried out an experimental investigation of the use of shot peening, laser peening and cavitation peening to improve the fatigue strength of Ti6Al4V manufactured by an electron beam melting method.

As is well known, additive manufacturing, which is also called direct manufacturing, such as by electron beam melting and/or selective laser melting, is suitable for the manufacture of medical implants, since porous implants can be produced and they can be made based on the needs of each individual patient. However, the fatigue strength and/or fatigue life of AM metals is much smaller than that of bulk materials because of the surface roughness. It has been reported that the fatigue life of titanium alloy Ti6Al4V produced by additive manufacturing, rolling and casting decreased as the maximum surface roughness increased [8].

Several methods, including electron beam melting (EBM), selective laser melting (SLM), laser engineered net shaping (LENS) and a wire feed method have been proposed [9,10]. The advantage of EBM is that the build rate is normally larger than that of SLM [9,11]. However, the fatigue strength of EBM materials is smaller than that of SLM materials [9,10,12], as the roughness of the surface is greater [10]. Thus, the main purpose of the present paper is to improve the fatigue strength of titanium alloy Ti6Al4V manufactured by EBM.

It has been reported that the fatigue strength and/or fatigue life of titanium alloy Ti6Al4V manufactured by EBM can be improved by shot peening and cavitation peening [2,3]. The conventional method for mechanically treating a surface is shot peening. As mentioned above, shot peening can improve the fatigue strength of AM metals [2,3]. However, shot peening produces dust due to collisions between the shot, and the dust causes dust explosions [13] and a health hazard. In order to avoid these risks, a shot peening technique using recirculating shot accelerated by a water jet was established [14]. This technique was used in this study for shot peening.

In the case of laser peening, there are two major methods. One method is to use a powerful pulsed laser, such as one with several J per pulse, to treat the surface, which is covered by a sacrificial layer of tape or paint. In this method, a liquid film is formed on the surface [4,6]. The other method is submerged laser peening which obviates the need for a sacrificial layer [5]. In either case, it is considered that a laser induced shock wave in the liquid results in the material being treated. As is well known, in the case of submerged laser peening, a bubble is generated after laser ablation, and this bubble develops, then collapses, and as its collapse it erodes the surface, the same as cavitation bubble [7]. Thus, in this paper, this process, which follows laser ablation, is called “laser cavitation”. Using a submerged shock wave sensor to measure the pressure amplitude in the water showed that the pressure induced by laser ablation was larger than that by laser cavitation [15]. However, when the force due to the impact was measured by a special homemade sensor developed to evaluate cavitation impact [16,17], the amplitude of the impact induced by laser cavitation was 1.5 times larger than that due to laser ablation [7]. That is, when laser cavitation is considered and optimized, we get two hits, i.e., from laser ablation and laser cavitation, with a single pulse. Thus, in

the present experiment, the submerged laser peening system was used.

In the case of cavitation peening, shots are not required. Thus chemical cleaning to remove material transferred to the surface from the shots is unnecessary. Moreover, since cavitation peening can be used to treat the inner walls of a tube by placing it parallel to the jet axis [18], it can be used in the manufacture of porous medical implants. It has been reported that the fatigue strength of spinal implants made of titanium alloy was improved by cavitation peening [19]. Note that the mechanism for cavitation peening is different to that of water jet peening, in which the impacts of water columns are used to create plastic deformation [20]. Even though the water jet is submerged, the surface can be treated by water jet peening. In the case of water jet peening, a powerful plunger pump with an injection pressure of several hundreds of MPa is required. On the other hand, in the case of cavitation peening, the injection pressure required for a cavitating jet is about one tenth of the pressure required for water jet peening [21]. Thus, risk of surface damage to the implants by cavitation peening is negligible compared to water jet peening, and also the initial and running costs of cavitation peening are less than one tenth of those of water jet peening. Thus, in the present experiments, the effect of cavitation peening using a submerged water jet was investigated.

As mentioned above, the impact mechanism to produce local plastic deformation is different for each peening method [20]. The impact of shot with the surface is used in shot peening, whereas the impact induced by laser ablation and laser cavitation are utilized for submerged laser peening, and the impact induced by cavitation bubbles collapsing is used in cavitation peening. Thus, the strain rate for each peening method is different. It has been reported that the plastic deformation in the material and the surface roughness are different when the strain rate of the peening method is different [22]. Thus it is worthwhile investigating the improvements made in the fatigue life and/or fatigue strength of the AM metals used for medical implants by the different peening methods.

In this study, to compare the improvements made in the fatigue strength of an AM metal manufactured by EBM by the various peening methods, we used fatigue test specimens made of titanium alloy Ti6Al4V. These specimens were treated by shot peening, submerged laser peening and cavitation peening, then assessed by a plate bending fatigue test. Note that all the test specimens were heat-treated to improve the fatigue strength, as the fatigue strength of specimens without heat-treatment was considerably smaller than that of heat-treated specimens.

2. Experimental apparatus and procedures

2.1. Titanium alloy Ti6Al4V manufacture by EBM

Figure 1 illustrates the geometry of the specimens used for the plate bending fatigue tests. All the specimens were manufactured by EBM. The powder used in the EBM process was made of Ti6Al4V and had an average diameter of about 75 μm. The spot size of the electron beam for selective melting was 0.2 mm in diameter, and the stacking pitch was 90 μm. The specimens, as shown in Figure 1, included 4 holes. The stacking was in the width direction. The width of the specimens at the center was 20 mm with radius of curvature of 45 mm. The thickness of the specimens was 2 ± 0.2 mm. The specimens were heat treated at 1208 K under vacuum for 105 minutes then cooled in argon. After that, aging was done at 978 K under vacuum for 2 hours, followed by argon gas cooling. In addition, the edges of all the specimens were polished by hand using rubber whetstones of #80 and #180, to reduce crack initiation from the edges.

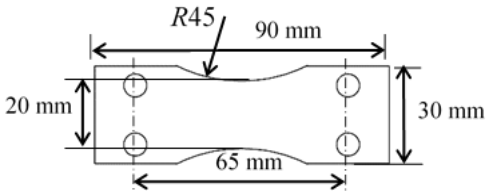

Figure 1. Dimensions of bending fatigue specimen (Thickness: 2 mm).

2.2. Shot peening apparatus

Figure 2 shows a schematic diagram of the shot peening system, in which the shots are accelerated by a water jet [14]. The shots were made of stainless steel Japanese Industrial Standards JIS SUS440C. The number and diameter of the shot were 500 and 3.2 mm, respectively. The water jet, with an injection pressure of 12 MPa, was injected into the chamber through three 0.58 mm diameter holes. The standoff distance between the nozzle and the specimen was 50 mm, and the diameter of the chamber was 54 mm. Without shot, no compressive residual stress was introduced into stainless steel, so, without shot, the water jet has scarcely any effect on the titanium alloy. The chamber was moved by a motor to uniformly treat the specimen surface. The processing time per unit length, t_p, is defined by the scanning speed, v, and the number of scans, n, as follows:

$$t_p = \frac{n}{v} \tag{1}$$

In the present experiment, t_p, was set to 1 s/mm considering the results of previous reports [3,23].

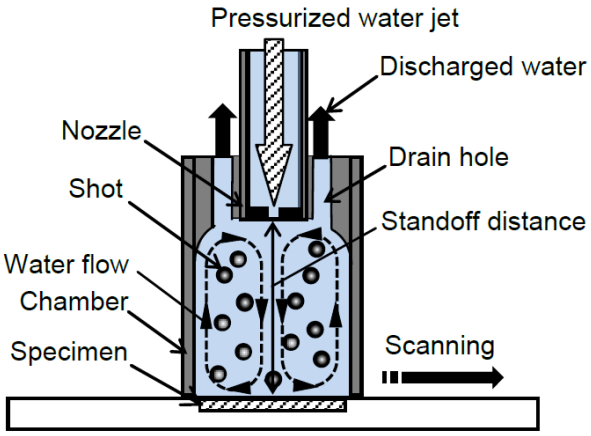

Figure 2. Schematic diagram of shot peening apparatus.

2.3. Laser peening apparatus

Figure 3 shows a schematic diagram of the submerged laser peening apparatus. A Q-switched Nd:YAG laser was used for the laser peening. The wavelength, maximum energy, beam diameter, pulse width and repetition frequency were 1064 nm, 0.35 J, 6 mm, 6 ns and 10 Hz, respectively. Normally, the second harmonic of a Nd:YAG laser, i.e., wavelength of 532 nm, is used for

submerged laser peening in order to mitigate absorption in the water [5]. As mentioned in the introduction, it was found that the impact produced by laser cavitation was larger than that produced by laser ablation [7]. From the point of view of the generation of laser cavitation, 1064 nm is better than 532 nm as the heat is more concentrated. When the standoff distance in water, s_w, is optimized, the submerged laser can introduce compressive residual stress into hard metals such as alloy tool steel [24]. On the other hand, 40% of the total power of the source is lost in obtaining the second harmonic. Thus, the fundamental harmonic, i.e., at 1064 nm, was used in the present experiment. The laser was focused on the specimen in the water filled hard glass chamber by a convex lens with a focal length of 100 mm. The standoff distance in air, s_a, and in water, s_w, were optimized by evaluating the peening intensity by measuring the arc height of an Almen strip at various values of s_a and s_w. In the present study, the values of s_a and s_w were chosen to be 84 mm and 19 mm, respectively. The diameter of the laser spot under these conditions was about 0.8 mm. The thickness of the glass of the chamber was 3 mm, and the length, width and height of the chamber were each 150 mm. The chamber was filled with deionized water, and deionized water was feed into the chamber at 5 liters per minute to remove particles in the water produced by ablation.

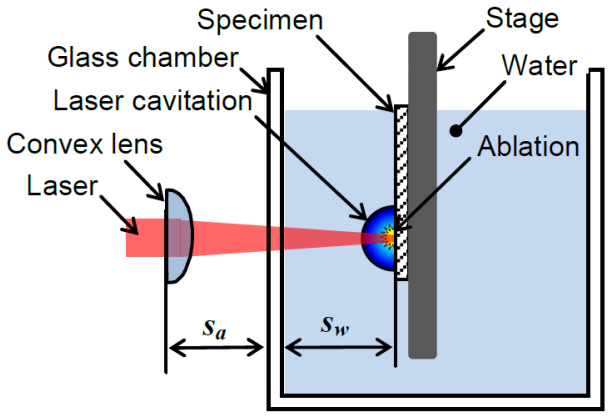

Figure 3. Schematic diagram of submerged laser peening apparatus.

The specimen was placed on a stage which was moved by stepping motors in the vertical and horizontal directions. The pulse density d_L was controlled by the horizontal speed v_h and stepwise movement in the vertical direction s_v was done by a stepping motor. As the repetition frequency of the laser was 10 Hz, d_L is given by the following equation:

$$d_L = \frac{10\,n}{v_h\,s_v} \tag{2}$$

In the present experiment, d_L, was set to 5 pulses/mm^2 considering the results of a previous report [23]. Values of n = 1, v_h = 4.46 mm/s, s_v = 0.448 mm were chosen.

2.4. Cavitation peening apparatus

Figure 4 shows a schematic diagram of the cavitating jet apparatus used. In this apparatus, a high speed water jet, pressurized by a plunger pump capable of producing a pressure of 30 MPa and a flow rate of 3 × 10^{-2} m^3/min, is forced into a water filled stainless steel tank through a nozzle.

When a high speed water jet such as this is driven into water, cloud cavitation is generated inside the nozzle and/or in the shear layer around the jet. A submerged water jet with cavitation is called a cavitating jet [7]. The cloud cavitation becomes ring vortex cavitation at the surface being treated, so that an annular ring is treated when the ring vortex collapses [25]. When the specimen is placed near the nozzle, a cavitating jet with high injection pressure also peens metallic materials in a limited region at the jet center due to the impact of the water column, the same as in water jet peening. However, the area treated by water jet peening is very small, being about 5 mm in diameter compared to 60 mm for cavitation peening, and water jet peening is less effective than cavitation peening [26]. Cavitation peening and water jet peening can be classified according to the standoff distance and the cavitation number σ [7]. In this study, the peening was carried out under cavitation peening conditions. The cavitation number σ depends on the upstream pressure of the nozzle, i.e., the injection pressure p_1, the downstream pressure p_2 and the vapor pressure of water p_v, and is given by:

$$\sigma = \frac{p_2 - p_v}{p_1 - p_2} \cong \frac{p_2}{p_1} \tag{3}$$

As $p_1 \gg p_2 \gg p_v$, σ can be simplified, as shown in Eq 3. For the experiments carried out for this study, the injection pressure p_1 was 30 MPa and the cavitation number σ was 0.0033. The standoff distance, s, is given by the distance between the upstream edge of the nozzle plate and the surface of the specimen. At σ = 0.0033 and with s greater than 111 mm, cavitation peening is obtained [7]. On the other hand, with σ = 0.0033 and s < 111 mm, water jet peening is obtained. For these experiments, s was set to 222 mm. Thus, cavitation peening was done in the present case.

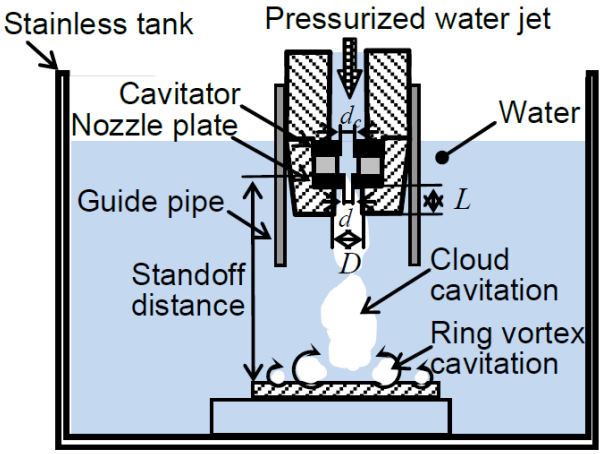

Figure 4. Schematic diagram of cavitation peening apparatus.

The nozzle throat diameter, d, was 2 mm and the thickness of the nozzle plate was 6 mm. In order to increase the intensity of the cavitating jet, the outlet bore diameter D and length L were optimized, with D = 16 mm and L = 16 mm [27], and a cavitator and a guide pipe [28] were installed in the nozzle assembly. The diameter of the cavitator, d_c, was 3 mm. The nozzle was set at about 0.3 m beneath the surface of the water to reduce the suction vortex. In these experiments, t_p, which is given by Eq 1, was set to 10 s/mm considering the results obtained in a previous study [23].

2.5. Evaluation of fatigue strength and mechanical properties

The fatigue life and strength was examined by a Schenk-type displacement-controlled plate bending fatigue tester at $R = -1$, as shown in Figure 5. The maximum bending moment of the tester was ±15 Nm and the span length at fixed point was 65 mm as shown in Figure 1. The test frequency was 12 Hz. The applied bending moment was monitored by a load cell, and when the bending moment became about 20% of applied bending moment, it was distinguished as failure. The applied bending stress σ_a was calculated from the thickness of the specimen, δ, measured by a digital caliper with an accuracy of 0.01 mm, and the applied moment M as follows.

$$\sigma_a = \frac{M}{\frac{1}{6}(b\delta^2)} \tag{4}$$

Here, b is the width at the center of the specimen where it fractured.

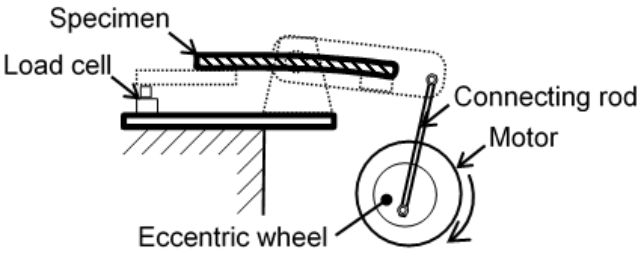

Figure 5. Schematic diagram of a Schenk-type displacement-controlled plate bending fatigue tester.

The profile of the specimen surface was evaluated using a stylus type profilometer in order to measure the arithmetical mean roughness R_a, the maximum height of the roughness profile R_z and the skewness R_{sk}. The specimen was also examined using a laser microscope and an optical microscope.

In order to make a clear comparison between the effects of the various peening methods on work hardening, the hardness was measured using a Rockwell superficial hardness tester, as the surfaces of specimens manufactured by EBM are very rough. The Rockwell superficial hardness was evaluated using a diamond indenter and a ball indenter with a diameter of 1/16" (1.59 mm) at an applied load of 147 N. The hardness measured by each of these is identified by *HR15N* and *HR15T*, respectively. In order to prevent the surface roughness from having an effect on the hardness test, the Vickers hardness of the surface of a test specimen peened after grinding was measured with a load of 1.96 N.

3. Results

3.1. Appearance and roughness of the peened surfaces

Figure 6 shows the surfaces of (a) non-peened, (b) cavitation peened, (c) laser peened and (d) shot peened specimens. As shown in Figure 6a, many partially melted particles can be seen on the surface. In the case of shot peening, the surface has been deformed by collisions with the shot. However, sharp valleys are still present on the shot peened surface. On the other hand, in the cases of

laser peening and cavitation peening, the particles are still evident. The wrinkles on the laser peened surface might be produced by partial melting by laser ablation. Furthermore, the laser peened surface has become darker due to the oxidized layer. On the cavitation peened surface, the number of particles seems to be less than the non-peened and laser peened specimens, which is due to incompletely bonded particles being removed by cavitation impact. Note that this cavitation peening has been reported as introducing compressive residual stress of 194 ± 34 MPa [3].

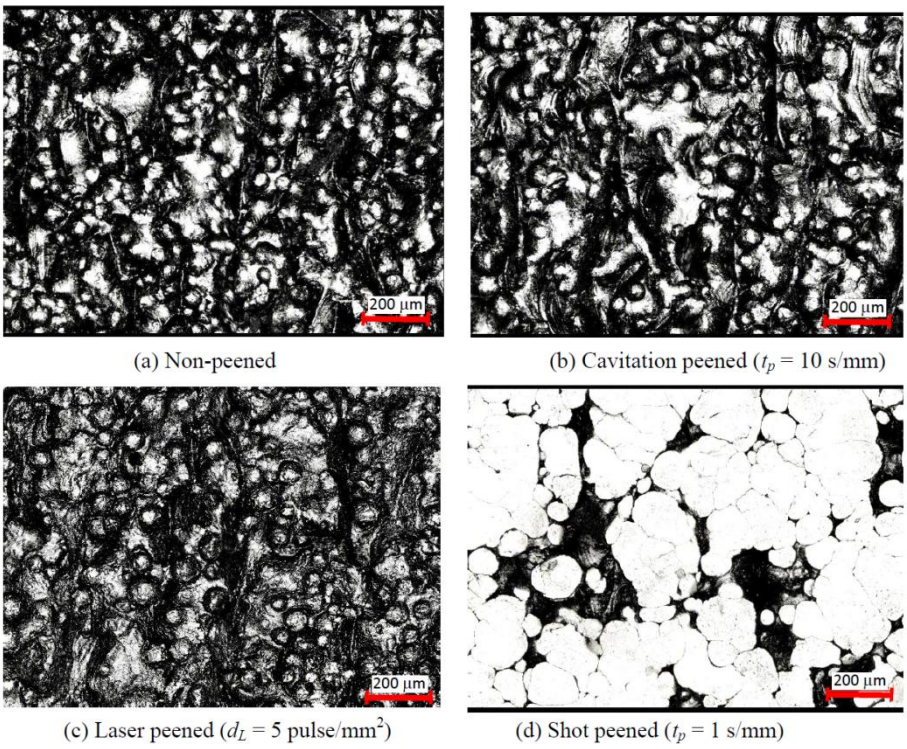

(a) Non-peened (b) Cavitation peened (t_p = 10 s/mm)

(c) Laser peened (d_L = 5 pulse/mm^2) (d) Shot peened (t_p = 1 s/mm)

Figure 6. Appearance of the surfaces of specimens viewed using a laser microscope.

Figure 7 shows the characteristics of the surfaces: (a) the arithmetical mean roughness R_a, (b) the maximum height of the roughness profile R_z and (c) the skewness R_{sk}. Standard deviations are shown by the horizontal bars. In Figure 7c, schematic profiles of typical cases for $R_{sk} > 0$ and $R_{sk} < 0$ are shown for reference. The cavitation peened surface is scarcely any different to that of a non-peened surface, as R_a, R_z and R_{sk} are nearly equal within the limits of the standard deviations. However, as mentioned above, compressive residual stress has been introduced by the cavitation peening [3]. In the case of laser peening, although R_a for laser peening is close to that of the non-peened specimen, R_z is slightly larger compared with the non-peened one. R_{sk} for laser peening is somewhat larger than those of the other specimens. In the case of both cavitation and shot peening, pits are randomly distributed. On the other hand, systematic peening by pulsed laser irradiation produces deeper and deeper valleys giving rise to a series of higher and higher peaks. This is why R_z for laser peening is larger than that of the other specimens and why R_{sk} for laser peening is positive. In the case of shot peening, the convex parts of the particles on the surface were flattened as shown in Figure 6d. Thus, R_a and R_z for shot peening decreased due to plastic deformation of the surface, and R_{sk} was much less than zero.

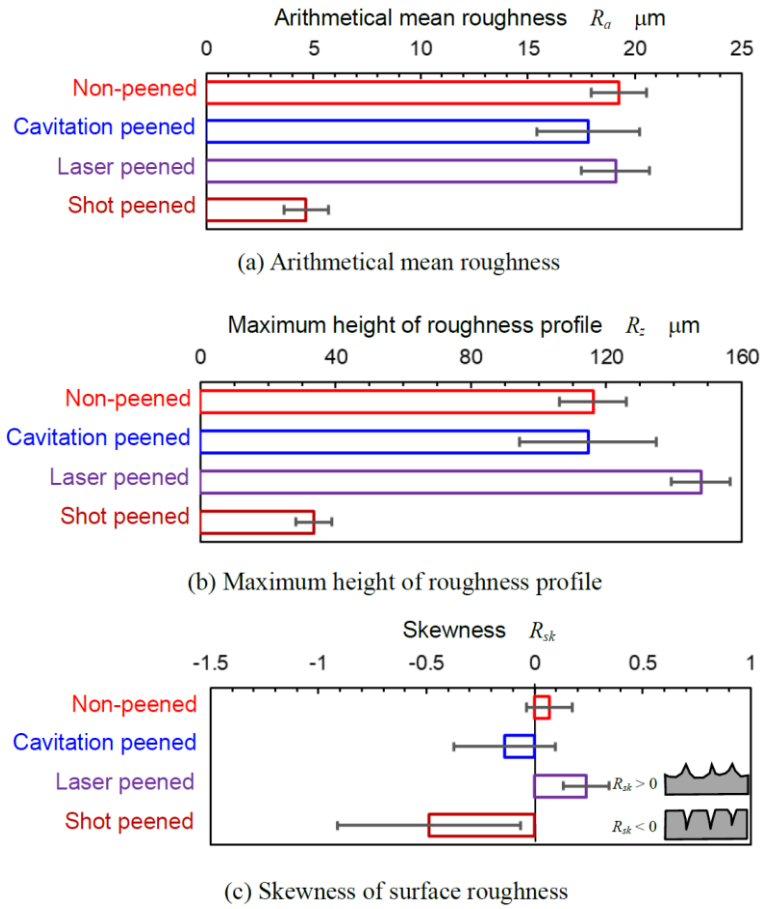

Figure 7. Surface roughness of the specimens.

The effect the various peening methods have on work hardening can be understood from Figure 8, which shows the Rockwell superficial hardness *HR15N* and *HR15T* of non-peened, cavitation peened, laser peened and shot peened specimens. In the case of *HR15N* the indenter is a circular cone, so the results for the non-peened specimen are scattered, but it was concluded that the order of decreasing hardness was by shot peening, cavitation peening, laser peening and without peening.

In the case of *HR15T*, the order of hardness was nearly the same as *HR15N*. As shown in Figure 8, *HR15T* for shot peening is much larger than for cavitation peening and laser peening. This tendency is caused by the differences in surface roughness. For the *HR15T* measurement, the initial load was 29.4 N and the applied test load was 147 N. As shown in Figures 6 and 7, the surfaces after cavitation peening and laser peening were very rough, whereas the shot peened surface was nearly flat with some valleys. Since the 1.59 mm diameter indenter with a load of 29.4 N did not reach the bottom surface of the cavitation and laser peened specimens, the movement of the indenter when the test load was applied was larger than that on a smooth surface. This is why *HR15T* for the shot peened specimen appears to be much larger than the other specimens.

In order to investigate work hardening by peening without the effect of surface roughness, the Vickers hardness of ground specimens were measured. The results are shown in Figure 9. Firstly, the surfaces of the as-manufactured specimens were mechanically finished by grinding. After grinding, specimens were treated by cavitation peening at t_p = 10 s/mm, laser peening at d_L = 5 pulse/mm^2 and shot peening at t_p = 1 s/mm, i.e., the same conditions as used previously. *HV* for the non-peened

specimen was 344 ± 6, whereas it was 367 ± 17 for the cavitation peened specimen, 338 ± 21 for the laser peened specimen and 386 ± 26 for the shot peened specimen. The cavitation and shot peened specimens were harder than the non-peened specimen, and the shot peened specimen was harder than the cavitation peened specimen under the present conditions. Note that the difference in *HV* is not as great as the difference in *HR15T*. That is, the values of *HR15T* were affected by the surface roughness as mentioned above. On the other hand, *HV* after laser peening is slightly smaller than that of the non-peened specimen. This might be caused by heat generated during laser ablation. It was concluded that shot peening and cavitation peening caused work hardening, and laser peening produced softening due to the heat.

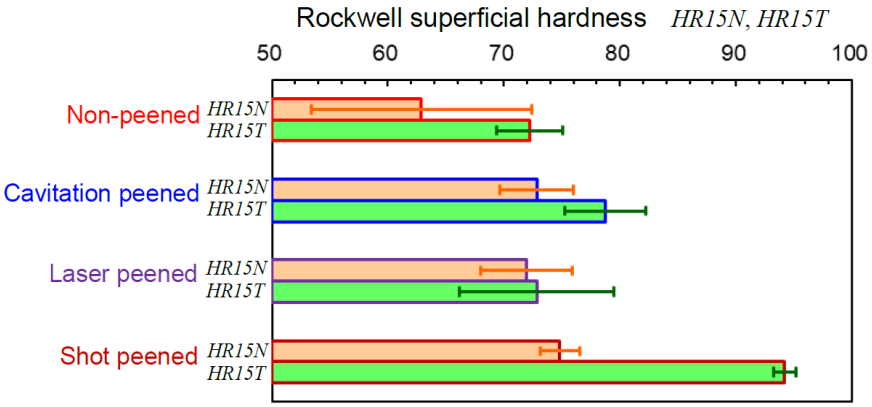

Figure 8. Rockwell superficial hardness of as-built specimens.

Figure 9. Vickers hardness of ground specimens.

3.2. Improving the fatigue strength by various peening methods

In order to demonstrate the improvements in fatigue life and strength by the various peening methods, Figure 10 shows the relationship between the amplitude of the bending stress and the number of cycles to failure, i.e., the *S–N* curve, for non-peened, cavitation peened, laser peened and shot peened specimens. The treatment conditions for each peening method are mentioned above. Figure 11 shows cracks propagating on the specimen surfaces during fatigue tests at $N \approx 3.2\text{~}5.1 \times 10^5$, and Figure 12 shows cross sectional views of the fractures. The white arrows in Figure 12 show which surfaces are shown in Figure 11. For these experiments, the edges of the specimens were rounded by hand using a rubber whetstone in order to mitigate crack initiation at the edges as mentioned in Section 2. As shown on the left hand side of Figure 11a, the two cracks have clearly started from the surface. The rounding method was applicable for these fatigue tests, as the datum

point for the non-peened specimen was on the curved line. As mentioned above, the laser peened surface was covered by an oxide layer so the surface is darker compared with the other specimens.

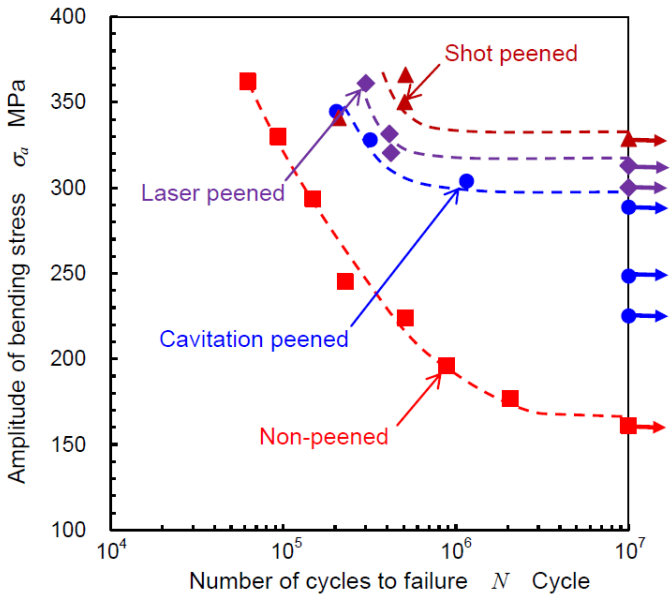

Figure 10. Comparison of the improvements made in the fatigue strength of Ti6Al4V manufactured by EBM by the various peening methods.

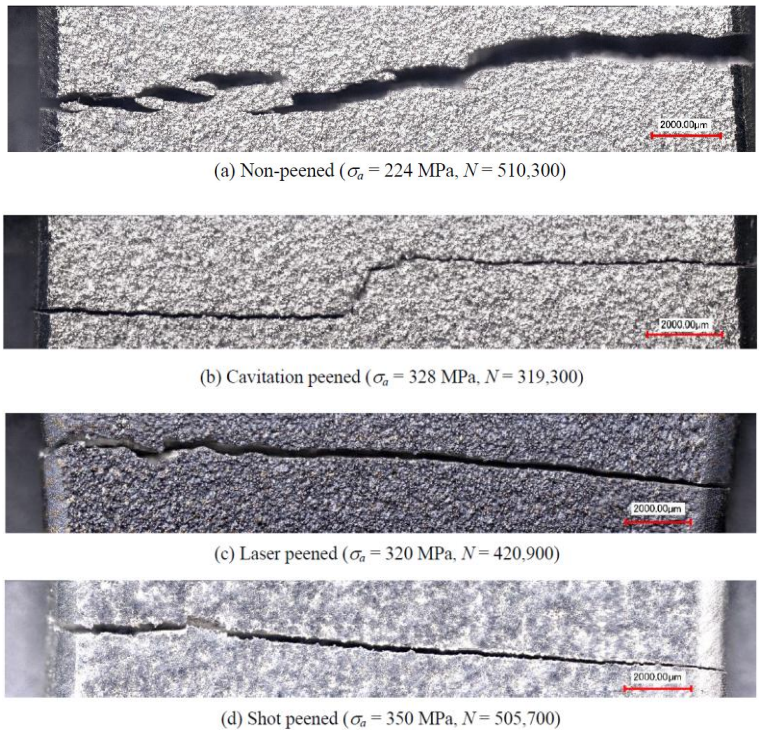

Figure 11. Crack propagation on the specimen surfaces.

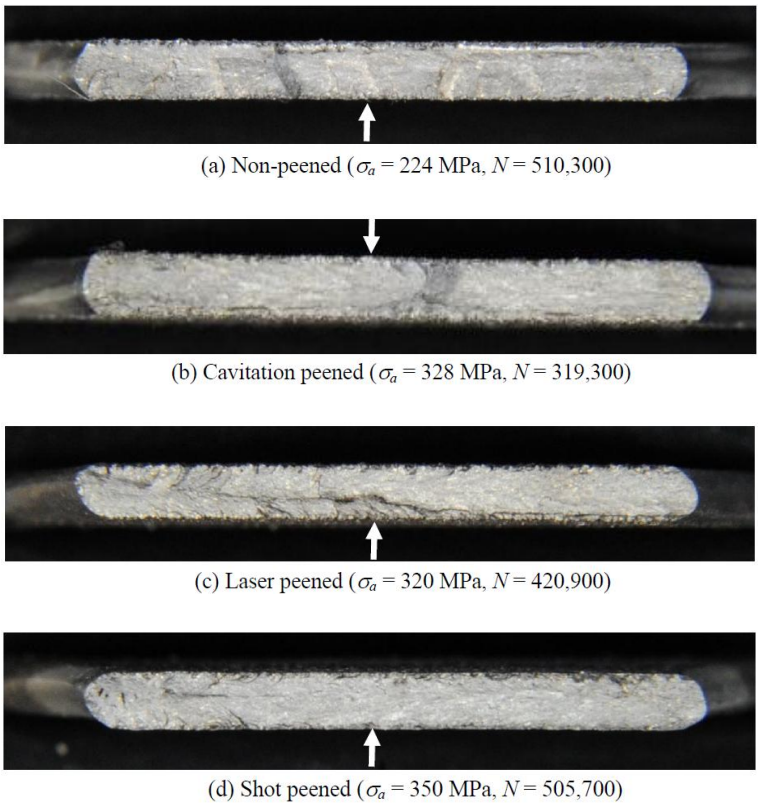

Figure 12. Cross sectional views of the fractured surfaces. The white arrows in Figure 12 depict which surfaces are shown in Figure 11.

As shown in Figure 10, all the peening methods improved the fatigue life and the strength, as the *S*–*N* curves of the peened specimens have shifted to the upper right. We calculated the fatigue strength by Little's method [29] and found it was 169 ± 8 MPa for the non-peened specimen, 296 ± 8 MPa for the cavitation peened specimen, 317 ± 4 MPa for laser peened specimen and 335 ± 6 MPa for shot peened specimen. That is, the fatigue strength of Ti6Al4V manufactured by EBM was improved by 75% by cavitation peening, 87% by laser peening and 98% by shot peening. Note that the fatigue strength of Ti6Al4V manufactured by EBM is much smaller than that of the bulk material, as previously reported [2,3]. Thus, it is worthwhile to treat Ti6Al4V by peening, as this almost doubles the fatigue strength.

4. Discussion

As shown in Figures 6, 11 and 12, the surfaces without peening, and after cavitation peening and laser peening are very rough because of the particles left by EBM. On the other hand, the shot peened surface was deformed by the shot. Thus, the surface roughness after shot peening was much smoother than that of the other surfaces. For these experiments, the amplitude of the bending stress was calculated using Eq 4, using the thickness δ_1 measured by a digital caliper for δ in Eq 4. Thus, δ_1 includes the thickness of the core part, δ_2, and the surface roughness, R_z, as shown in Figure 13. The relationship between δ_1, δ_2 and R_z is given by Eq5 below. During the fatigue test, the bending moment M is applied to the core part only, so the actual amplitude of the bending stress σ_a' was

re-calculated using the thickness of the core part, δ_2, for δ in Eq 4. This enables us to investigate the actual fatigue strength.

$$\delta_2 = \delta_1 - 2Rz \tag{5}$$

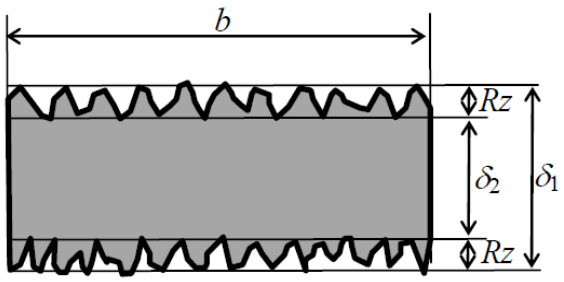

Figure 13. Schematic diagram of a cross sectional view of a specimen for calculating the bending stress.

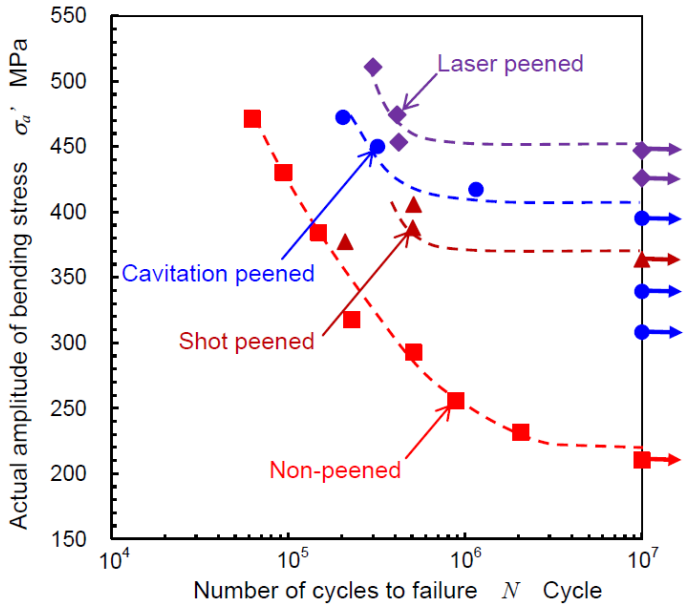

Figure 14. *S–N* curves using the actual amplitude of the bending stress.

Although the notch effect also affects fatigue strength, it was assumed that this would be the same for all the peening conditions. Figure 14 shows the relationship between the actual amplitude of the bending stress σ_a' and the number of cycles to failure *N*. The data are the same as in Figure 10, except the bending stress has been recalculated. Thus, since $\delta_2 < \delta_1$, then $\sigma_a' > \sigma_a$. The differences between Figure 10 and Figure 14 are remarkable as they show that the fatigue strength after laser peening and cavitation peening is greater than that after shot peening. This is because R_z after laser peening and cavitation peening are larger than that after shot peening. Using Little's method [29] to recalculate the fatigue strength gave 221 ± 11 MPa for the non-peened specimen, 406 ± 11 MPa after cavitation peening, 450 ± 3 MPa after laser peening and 371 ± 7 MPa after shot peening. Thus, the fatigue strength of Ti6Al4V manufactured by EBM was improved by 84% by cavitation peening, 104% by laser peening and 68% by shot peening. That is, when the actual bending stress was

considered, the improvement by laser peening was greater than that by shot peening. Whichever of these mechanical surface treatments is used, the fatigue strength of Ti6Al4V manufactured by EBM is nearly doubled. Note that cavitation peening may be more suitable for improving the fatigue strength of porous medical implants, since cavitation bubbles can pass thought the narrow pores and impact with the surfaces of the pores. When the fatigue strength at 10^7 of bulk material made of Ti6Al4V with heat treatment was calculated using data of literature [30], the fatigue strength was 545 ± 10 MPa. Note that Vickers hardness of Ti6Al4V in the reference [30] was 326. Namely, the fatigue strength of tested Ti6Al4V manufactured EBM was about 40% of the bulk Ti6Al4V, and it was improved up to 80% of the bulk Ti6Al4V by proposed laser peening.

5. Conclusions

In order to demonstrate the improvement various peening methods have on the fatigue strength of medical implants made by additive manufacturing, titanium alloy Ti6Al4V manufactured by EBM was treated by shot peening, laser peening and cavitation peening. The fatigue strength of the peened specimens and a non-peened specimen was investigated by a plate bending fatigue test. Shot peening was carried out using a recirculating shot peening system, in which the shot were accelerated by a water jet with an injection pressure of 12 MPa, in order to remove the dust generated during shot peening. For laser peening, a submerged laser peening system with a laser energy of 0.35 J and wavelength of 1064 nm was used. This utilizes the laser cavitation impact which develops after laser ablation. A submerged water jet with an injection pressure of 30 MPa was used for the cavitation peening. The results obtained can be summarized as follows:

(i) Shot peening, laser peening and cavitation peening all improved the fatigue strength and fatigue life of Ti6Al4V manufactured by EBM.

(ii) The fatigue strength of Ti6Al4V was doubled by shot peening, when the thickness including the surface roughness was used to calculate the bending stress. Under the experimental conditions used here, the fatigue strength was improved by 75% by cavitation peening, 87% by laser peening and 98% by shot peening.

(iii) When the surface roughness was taken into account and the actual bending stress was used to evaluate the fatigue strength, the improvement in fatigue strength by laser peening was greater than that by shot peening. In this case, the fatigue strength of Ti6Al4V was improved by 84% by cavitation peening, 104% by laser peening and 68% by shot peening. Since the surface roughnesses of the AM metal specimens was quite large and different for each specimen, it is more appropriate to use the actual stress applied to the specimens in calculating the fatigue strength.

(iv) When Ti6Al4V manufactured by EBM is heat treated and aged, the fatigue strength is still very small compared with the bulk material. Thus, it is worthwhile treating the surfaces of AM metals by a mechanical surface treatment, as the fatigue strength can be doubled by peening.

Acknowledgments

This work was partly supported by JSPS KAKENHI Grant Number 17H03138. The authors wish to thank Mr. M. Mikami, Technician in the Department of Finemechanics, Tohoku University for his help in the experiments.

Conflict of interest

The authors declare no conflict of interest.

Author contributions

H.S. conceived and designed the experiments; H.S. and Y.O. performed the treatment and evaluated the samples; H.S. performed the fatigue tests and wrote the paper.

References

1. Murr LE, Gaytan SM, Medina F, et al. (2010) Next-generation biomedical implants using additive manufacturing of complex, cellular and functional mesh arrays. *Philos T R Soc A* 368: 1999–2032.
2. Edwards P, O'Conner A, Ramulu M (2013) Electron beam additive manufacturing of titanium components: Properties and performance. *J Manuf Sci E-T ASME* 135: 061016.
3. Sato M, Takakuwa O, Nakai M, et al. (2016) Using cavitation peening to improve the fatigue life of titanium alloy Ti-6Al-4V manufactured by electron beam melting. *Mater Sci Appl* 7: 181–191.
4. Peyre P, Fabbro R, Merrien P, et al. (1996) Laser shock processing of aluminium alloys. Application to high cycle fatigue behaviour. *Mat Sci Eng A-Struct* 210: 102–113.
5. Sano Y, Obata M, Kubo T, et al. (2006) Retardation of crack initiation and growth in austenitic stainless steels by laser peening without protective coating. *Mat Sci Eng A-Struct* 417: 334–340.
6. Hatamleh O, Lyons J, Forman R (2007) Laser and shot peening effects on fatigue crack growth in friction stir welded 7075-T7351 aluminum alloy joints. *Int J Fatigue* 29: 421–434.
7. Soyama H (2017) Key factors and applications of cavitation peening. *Int J Peen Sci Technol* 1: 3–60.
8. Chan KS, Koike M, Mason RL, et al. (2013) Fatigue life of titanium alloys fabricated by additive layer manufacturing techniques for dental implants. *Metall Mater Trans A* 44: 1010–1022.
9. Herzog D, Seyda V, Wycisk E, et al. (2016) Additive manufacturing of metals. *Acta Mater* 117: 371–392.
10. Cao F, Zhang TT, Ryder MA, et al. (2018) A review of the fatigue properties of additively manufactured Ti-6Al-4V. *JOM* 70: 349–357.
11. Zhao XL, Li SJ, Zhang M, et al. (2016) Comparison of the microstructures and mechanical properties of Ti-6Al-4V fabricated by selective laser melting and electron beam melting. *Mater Design* 95: 21–31.
12. Fousova M, Vojtech D, Doubrava K, et al. (2018) Influence of inherent surface and internal defects on mechanical properties of additively manufactured Ti6Al4V alloy: Comparison between selective laser melting and electron beam melting. *Materials* 11: 537.
13. Abbasi T, Abbasi SA (2007) Dust explosions—Cases, causes, consequences, and control. *J Hazard Mater* 140: 7–44.
14. Naito A, Takakuwa O, Soyama H (2012) Development of peening technique using recirculating shot accelerated by water jet. *Mater Sci Technol* 28: 234–239.

15. Sasoh A, Watanabe K, Sano Y, et al. (2005) Behavior of bubbles induced by the interaction of a laser pulse with a metal plate in water. *Appl Phys A-Mater* 80: 1497–1500.
16. Soyama H, Lichtarowicz A, Momma T, et al. (1998) A new calibration method for dynamically loaded transducers and its application to cavitation impact measurement. *J Fluids Eng* 120: 712–718.
17. Soyama H, Sekine Y, Saito K (2011) Evaluation of the enhanced cavitation impact energy using a PVDF transducer with an acrylic resin backing. *Measurement* 44: 1279–1283.
18. Soyama H (2016) Opposed cavitating jets and their application for cavitation peening of wall surrounding hole. *Proceedings of 23rd International Conference on Water Jetting*, 201–208.
19. Takakuwa O, Nakai M, Narita K, et al. (2016) Enhancing the durability of spinal implant fixture applications made of Ti-6Al-4V ELI by means of cavitation peening. *Int J Fatigue* 92: 360–367.
20. Soyama H (2015) Surface mechanics design of metallic materials on mechanical surface treatments. *Mech Eng Rev* 2: 14-00192.
21. Soyama H, Nagasaka K, Takakuwa O, et al. (2012) Optimum injection pressure of a cavitating jet for introducing compressive residual stress into stainless steel. *J Power Energy Syst* 6: 63–75.
22. Kanou S, Takakuwa O, Mannava SR, et al. (2012) Effect of the impact energy of various peening techniques on the induced plastic deformation region. *J Mater Process Tech* 212: 1998–2006.
23. Soyama H (2018) Effect of peening methods on improvement of fatigue strength of stainless steel by mechanical surface treatment. *Proceedings of 67th JSMS Annual Meetings*, 281–282.
24. Soyama H (2017) Introduction of compressive residual stress into alloy tool steel by submerged laser peening utilizing laser cavitation impact. *Proceedings of the 9th International Conference on Leading Edge Manufacturing in 21st Century, LEM 2017*, article number 010.
25. Soyama H, Yamauchi Y, Adachi Y, et al. (1995) High-speed observations of the cavitation cloud around a high-speed submerged water-jet. *JSME Int J B* 38: 245–251.
26. Kamisaka H, Soyama H (2018) Effect of injection pressure on mechanical surface treatment using a submerged water jet. *J Jet Flow Eng* 33: 4–10.
27. Soyama H (2011) Enhancing the aggressive intensity of a cavitating jet by means of the nozzle outlet geometry. *J Fluids Eng* 133: 101301.
28. Soyama H (2014) Enhancing the aggressive intensity of a cavitating jet by introducing a cavitator and a guide pipe. *J Fluid Sci Technol* 9: 13-00238.
29. Little RE (1972) Estimating the median fatigue limit for very small up-and-down quantal response tests and for S-N data with runouts. *ASTM STP* 511: 29–42.
30. National Institute for Materials Science Japan (2004) Data sheet on giga-cycle fatigue properties of Ti-6Al-4V (900 MPa class) titanium alloy. NIMS Fatigue Data Sheet No 92, 1–12.

AIMS Press